ELSEVIER

Journal of Photochemistry and Photobiology A: Chemistry 128 (1999) 1–13

Journal of
Photochemistry
and
Photobiology
A:Chemistry

www.elsevier.nl/locate/jphotochem

Photochemistry of nitrite and nitrate in aqueous solution: a review

John Mack, James R. Bolton *

Department of Chemistry, The University of Western Ontario, London, Ont., Canada, N6A 5B7

Received 22 March 1999; accepted 23 June 1999

Abstract

It has long been known that the photolysis of nitrite and nitrate solutions results in the formation of $^\bullet$OH radicals. The mechanism of NO_3^- photolysis has been the subject of considerable controversy in the literature, however. This review summarizes the experimental work on NO_2^- and NO_3^- photolysis in the context of recent advances in the understanding of the chemistry of the peroxynitrite anion ($ONOO^-$) in biological experiments. $ONOO^-$ has been found to play a far more significant role in the overall reaction mechanism of NO_3^- photolysis than had previously been suspected. Research on NO_2^- and NO_3^- photolysis, as a pathway to the destruction of organic contaminants in natural waters, is summarized. The possible impact of NO_2^- and NO_3^- on Advanced Oxidation Technologies (AOTs), in which $^\bullet$OH radicals are used to initiate the destruction of hazardous organic pollutants in drinking water and industrial waste streams, is explored. ©1999 Elsevier Science S.A. All rights reserved.

Keywords: Nitrite ion; Nitrate ion; Hydroxyl radical; Peroxynitrite; Photolysis; AOT

---

1. Introduction

The destruction of hazardous organic pollutants in waste streams can be achieved through the use of Advanced Oxidation Technologies (AOTs) [1]. AOTs usually involve highly reactive free radical species, such as the $^\bullet$OH radical [2], which initiate rapid reactions with organic compounds, either by addition to a double bond or through abstraction of a hydrogen atom from aliphatic compounds or side groups. The resulting organic radicals then react with oxygen to initiate a series of degradative oxidation reactions ultimately resulting in complete mineralization to CO_2 and H_2O. Currently, many commercial AOT installations utilize the UV photolysis of H_2O_2 to produce $^\bullet$OH radicals:

$$H_2O_2 \xrightarrow{h\nu} 2^\bullet OH \qquad (1)$$

The use of reaction (1) as a source of $^\bullet$OH is limited by the comparatively low molar absorption coefficients ($\varepsilon < 200\,M^{-1}\,cm^{-1}$) of H_2O_2 in the 200–300 nm region; however, this can usually be overcome by an adequate concentration of H_2O_2 and/or a longer pathlength [1]. The absorption spectra of NO_2^- [3] and NO_3^- [4,5] are dominated by intense $\pi \rightarrow \pi^*$ bands at 205 nm ($\varepsilon = 5500\,M^{-1}\,cm^{-1}$) and 200 nm ($\varepsilon = 9900\,M^{-1}\,cm^{-1}$), respectively (Fig. 1). The presence of these anions could therefore result in a significant ‘inner filter’ effect that could reduce the fraction of the incident UV-flux absorbed by H_2O_2. On the other hand, the photolysis of NO_2^- or NO_3^- is also known to result in the formation of $^\bullet$OH [6]. It has therefore been proposed that nitrite/nitrate photolysis [4,7–22] could be used to generate $^\bullet$OH for use in AOTs [12,23].

Gonzalez and Braun [24,25] recently reported the effect of H_2O photolysis on aqueous NO_2^- and NO_3^- solutions during irradiation in the vacuum-UV at 172 nm. In contrast, we focus on the impact of UV-irradiation in the output range ($\lambda > 200$ nm) of the medium pressure mercury lamps used in most commercial AOT operations. Since H_2O does not absorb significantly at $\lambda > 200$ nm, nitrite/nitrate photolysis is the primary source of $^\bullet$OH in the research covered by this review. The absorption spectra of NO_2^- and NO_3^- contain weak $n \rightarrow \pi^*$ bands at 360 nm ($\varepsilon = 22.5\,M^{-1}\,cm^{-1}$) and 310 nm ($\varepsilon = 7.4\,M^{-1}\,cm^{-1}$), respectively, which can absorb solar radiation ($\lambda > 295$ nm). As a result, many studies have been conducted on the significance of nitrite/nitrate photolysis as a degradation pathway for organic pollutants in natural waters [18,21,26–38]. The mechanism of nitrite/nitrate photolysis has also been the subject of detailed investigation [4,6,12–17,39–45] and the reactions of many of the daughter radicals have been explored [11,12,34–36,46–61]. The aims of this review are to provide a critical summary of current

---

* Corresponding author. Tel.: +1-519-661-2170; fax: +1-519-661-3022
E-mail address: jbolton@julian.uwo.ca (J.R. Bolton)

1010-6030/99/$ – see front matter ©1999 Elsevier Science S.A. All rights reserved.
PII: S1010-6030(99)00155-0

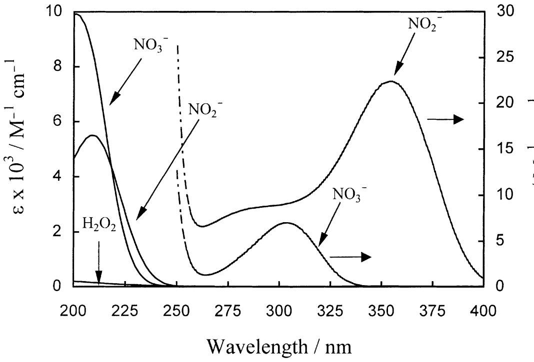

Fig. 1. The UV-visible absorption spectra of NO_2^-, NO_3^- and H_2O_2. The solid lines refer to the left *y*-axis and the broken lines refer to the right *y*-axis.

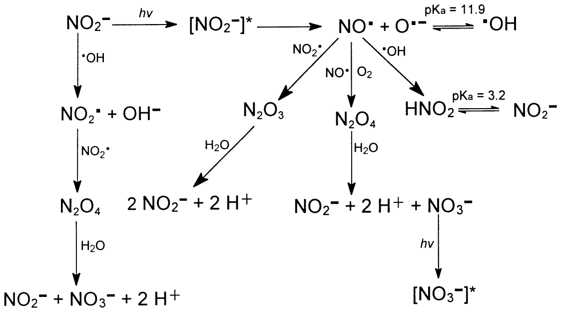

Scheme 1. Primary photoprocesses and subsequent reactions during NO_2^- photolysis. The reactions of the NO_3^- generated are not included but can be found in Scheme 2.

knowledge concerning NO_2^- and NO_3^- photolysis and to assess their impact on photochemically based AOTs.

2. Photolysis of Nitrite

The photolysis of NO_2^- in the 200–400 nm region results in the formation of $NO^\bullet$ and $O^{\bullet -}$ (see Scheme 1) [6–10,12,39]:

$$NO_2^- \xrightarrow{h\nu} [NO_2^-]^* \tag{2}$$

$$[NO_2^-]^* \rightarrow NO^\bullet + O^{\bullet -} \tag{3}$$

At $pH < 12$, $O^{\bullet -}$ protonates to form the $^\bullet OH$ radical ($pK_a = 11.9$ [14,62]).

$$O^{\bullet -} + H_2O \rightleftharpoons {}^\bullet OH + OH^- \quad k_4 = 1.7 \times 10^6\,M^{-1}\,s^{-1},\quad k_{-4} = 1.2 \times 10^{10}\,M^{-1}\,s^{-1} \tag{4}$$

The experimental Φ_{OH} values are listed in Table 1. The recombination reaction of the $^\bullet NO$ and $^\bullet OH$ radicals and the reaction of $^\bullet OH$ with NO_2^- are both essentially diffusion controlled reactions [24,25,62]:

$$NO^\bullet + {}^\bullet OH \rightarrow HNO_2 \quad k_5 = 1.0 \times 10^{10}\,M^{-1}\,s^{-1} \tag{5}$$

$${}^\bullet OH + NO_2^- \rightarrow NO_2^\bullet + OH^- \quad k_6 = 1.0 \times 10^{10}\,M^{-1}\,s^{-1} \tag{6}$$

These reactions therefore greatly limit the steady-state concentration of $^\bullet OH$ available to take part in oxidation reactions with organic pollutants. The mechanism of nitrite photolysis has been investigated by flash photolysis [6,7]. The $NO_2^\bullet$ formed in reaction (6) can react with $NO^\bullet$ to form N_2O_3 [24,25]:

$$NO^\bullet + NO_2^\bullet \rightarrow N_2O_3 \quad k_7 = 1.1 \times 10^9\,M^{-1}\,s^{-1} \tag{7}$$

N_2O_3 hydrolyses to regenerate NO_2^-:

$$N_2O_3 + H_2O \rightarrow 2\,H^+ + 2\,NO_2^- \quad k_8 = 5.3 \times 10^2\,s^{-1} \tag{8}$$

The $NO_2^\bullet$ radical can also dimerize during flash photolysis experiments to form N_2O_4 [24,25]:

$$2\,NO_2^\bullet \rightarrow N_2O_4 \quad k_9 = 4.5 \times 10^8\,M^{-1}\,s^{-1} \tag{9}$$

which hydrolyses to form NO_2^- and NO_3^- [24,25]:

$$N_2O_4 + H_2O \rightarrow NO_2^- + NO_3^- + 2\,H^+ \quad k_{10} = 1 \times 10^3\,s^{-1} \tag{10}$$

In solutions containing dissolved O_2, $NO^\bullet$ is competitively oxidized to form NO_3^- via N_2O_4 [12].

$$NO^\bullet + NO^\bullet \rightarrow N_2O_2 + O_2 \rightarrow N_2O_4 \tag{11}$$

The transient absorption spectra of $NO_2^\bullet$, N_2O_4 and N_2O_3 have all been identified [39]. Fischer and Warneck [22] added N_2O to a NO_2^- solution to assess whether hydrated electrons are also formed as a primary product of the photolysis of NO_2^- in the 280–390 nm region. The results were inconclusive.

3. Photolysis of nitrate

The overall reaction resulting from NO_3^- photolysis is (see Scheme 2) [13–17,40–42,63]:

$$NO_3^- \xrightarrow{h\nu} NO_2^- + \tfrac{1}{2}O_2 \tag{12}$$

In the absence of $^\bullet OH$ scavengers, this stoichiometry is said to be maintained over the entire pH range during irradiation with $\lambda > 200$ nm [13,15]. Isotope enrichment studies have indicated that NO_3^- is the origin of both O atoms in the O_2 generated [17]. Irradiation at $\lambda > 280$ nm is believed to result in two primary photolytic pathways [11,13,19,21]:

$$[NO_3^- \xrightarrow{h\nu} NO_3^-]* \tag{13}$$

$$[NO_3^-]^* \rightarrow NO_2^- + O(^3P) \tag{14}$$

$$[NO_3^-]^* \rightarrow NO_2^\bullet + O^{\bullet -} \xrightarrow{H_2O} NO_2^\bullet + {}^\bullet OH + OH^- \tag{15}$$

Warneck and Wurzinger [19] reported that $\Phi_O(^3P)$ is 0.1% and Φ_{OH} is 0.9% during irradiation at 305 nm (Tables 3 and

Table 1
Hydroxyl radical quantum yield data for nitrite photolysis

$[NO_2^-]$ (mM)	$^\bullet$OH Scavenger (technique)	λ (nm)	T (K)	pH	$\Phi_{(OH)}$ (%)	Reference
3	SCN^-	351	278	8	2.7 ± 0.3	[10]
	(UV–VIS)		288		3.8 ± 0.4	
			298		4.6 ± 0.3	
			308		5.8 ± 0.2	
			318		7.8 ± 0.3	
			328		9.1 ± 1.0	
			338		9.6 ± 0.3	
			348		11.8 ± 0.8	
			358		15.3 ± 0.9	
		308	278	6–9	3.9 ± 0.5	
			298		6.9 ± 0.9	
			318		8.1 ± 1.1	
			353		14.0 ± 0.7	
20	C_2H_5OH, $HCOO^-$	253.7	n.a.	1.4	4.6 ± 1.0	[11]
	(HPLC)	365			4.5 ± 1.0	
1.3	SCN^-	298.5	296 ± 2	7	5.3	[8]
	(UV–VIS)		296 ± 2	6	6.0	
			310	7.9	7.4	
			322	7.9	8.5	
	SCN^-	337.1	296 ± 2	6	6.4	
	SCN^-	354.6	296 ± 2	6.7	2.8	
					2.0	
					2.3	
	SCN^-	371.1	296 ± 2	6.7	1.8	
				7.9	1.3	
				8.7	1.4	
0.5	8 mM benzene	280	295	6.1	6.8	[22]
	(HPLC)	300			6.7	
		320			5.4	
		340			3.8	
		355			2.5	
		370			2.1	
		390			2.5	
		280	274	2.0	34.7	
		300			36.2	
		320			34.6	
		337.5			37.1	
		346.5			35.5	
		357.5			31.7	
		371			32.7	
		385.5			36.6	

4). A third primary reaction pathway is believed to result in the formation of the peroxynitrite anion ($ONOO^-$) via isomerization of $[NO_3^-]^*$ during irradiation at $\lambda < 280$ nm (see below) [13–16,43–45,64,65]:

$$[NO_3^-]^* \rightarrow ONOO^- \leftrightharpoons HOONO \quad pK_a = 6.5 \tag{16}$$

There is a second pathway to $ONOO^-$, since the radicals formed in reaction (15) can recombine within the solvent cage to form peroxynitrous acid (HOONO) [13,25,42,62]:

$$^\bullet OH + NO_2^\bullet \rightarrow HOONO \quad k_{17} = 1.3 \times 10^9\ M^{-1}s^{-1} \tag{17}$$

The reaction (17) will also occur in the bulk solution in deionized water, but this is unlikely to be a significant factor in natural waters or in the presence of $^\bullet$OH scavengers. At $pH < 7$, HOONO isomerizes rapidly to NO_3^- [13], and k_{18} is relatively independent of pH (a value of approximately $1.4\ s^{-1}$ [66] was recently reported):

$$HOONO \rightarrow NO_3^- + H^+ \tag{18}$$

Between pH 7 and 12, however, k_{18} drops by over five orders of magnitude, since $ONOO^-$ is relatively stable in solution [65]. The mechanism of reaction (18) is the subject of major controversy (see below), but it is possible that the homolysis of HOONO results in a 32% yield of $^\bullet$OH [67]. No evidence for the formation of solvated electrons or $NO_3^\bullet$ of major controversy (see below), but it is possible that the homolysis of HOONO results in a 32% yield of $^\bullet$OH [67]. No evidence for the formation of solvated electrons or $NO_3^\bullet$ radicals was found during studies involving irradiation at $\lambda > 200$ nm [16], but these species are formed at $\lambda < 190$ nm when H_2O is photolyzed [24,25]. H_2O_2 has not been detected as a significant product during steady-state irradiation of NO_2^- and NO_3^- solutions at $\lambda > 200$ nm [14,15,42]. The combination reaction between two $^\bullet$OH radicals is highly unlikely due

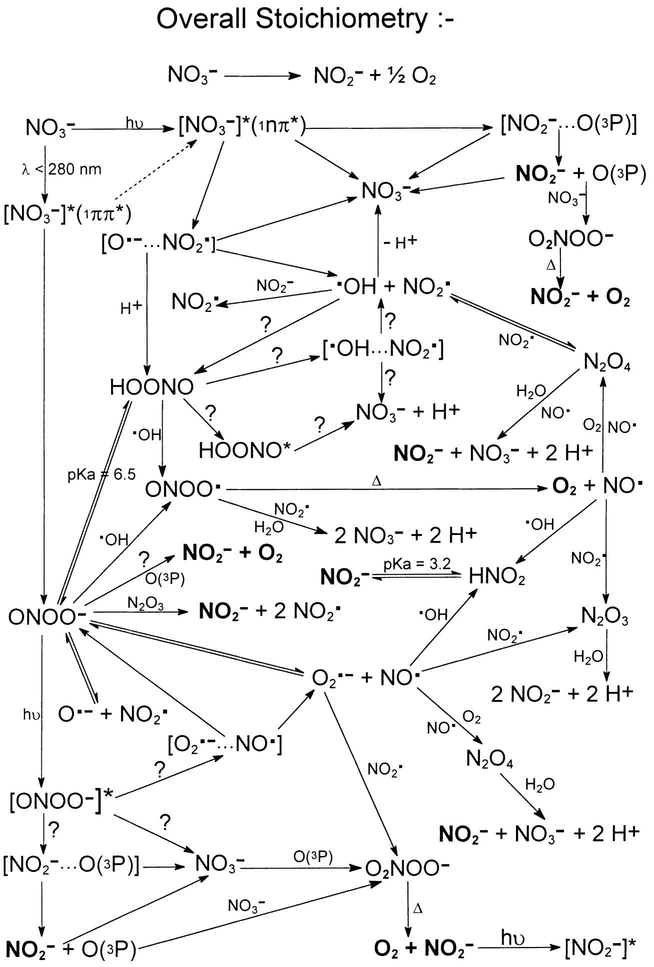

Scheme 2. Primary photoprocesses and subsequent reactions during NO_3^- photolysis. The reactions of the NO_2^- generated are not included but can be found in Scheme 1. Caged radical pairs are indicated by square brackets. The reactions of the NO_2^- generated are not included but can be found in Scheme 1.

to the very low concentration and short lifetime of $^\bullet$OH. Wagner et al. [13] have claimed that H_2O_2 formation is a viable reaction pathway in flash photolysis experiments. Since the lamp used to irradiate the solutions in that study had a very wide spectral output ($\lambda > 180$ nm), the H_2O_2 was probably formed via H_2O photolysis.

3.1. *The role of $OONO^-$ in NO_2^- formation*

The mechanism of NO_3^- photolysis has been the subject of considerable controversy in the literature, since many of the experimental observations are difficult to explain [13,42]. Daniels et al. [14] found that $\Phi_{NO_2^-}$ rises rapidly toward high pH in two steps for pH 8–10 and then for pH 11–13 during irradiation at 300 nm. Mark et al. [42] and Shuali et al. [15] observed similar results during irradiation at $\lambda < 280$ nm. The $\Phi_{NO_2^-}$ data for NO_3^- photolysis reported in the literature are summarized in Table 2. The most likely explanation is that an acid is involved in the reaction mechanism, which reacts more readily to form NO_2^- when it is deprotonated at high pH [13,17,42]. The most obvious candidate is HOONO, since the rise in $\Phi_{NO_2^-}$ closely matches the drop in the efficiency of reaction (18) [40,41,65]. This would require a reaction pathway that leads to the formation of NO_2^- and O_2 from $ONOO^-$; however, until recently, it had generally been assumed that reaction (18) was the only significant decomposition reaction for $ONOO^-$ during NO_3^- photolysis [40,41,63].

Table 2
Photolysis of nitrate: quantum yield of nitrite formation

$[NO_3^-]$ (M)	Technique	λ (nm)	T (K)	pH	$\Phi(NO_2^-)$ (%)	Reference
	UV–VIS	207		11.5	25	[17]
		254			17	
		282			2.4	
1.0	UV–VIS	229	293	11.7	23	[20]
		254			17	
		313			2.1	
0.01	UV–VIS	305	295 ± 2	5.6	0.59	[19]
0.1–0.2	UV–VIS	253.7	298		8.8 ± 0.8	[11]
		310			0.65 ± 0.04	
		313			0.63 ± 0.04	
0.01	IC	254	298	5	0.6	[42]
				13	10	

From the late 1960's until the early 1990's it was generally believed that the flash photolysis data reported by Barat et al. [15,64] had proven conclusively that $ONOO^-$ and NO_2^- are formed via independent pathways, since $ONOO^-$ was observed to form gradually over 60 μs. The data in this study are probably not reliable, however, since no filters were used in these experiments. The $ONOO^-$ formation was probably initiated by H_2O homolysis at $\lambda < 200$ nm, as has recently been reported by Gonzalez and Braun [24]. A number of different species were proposed to account for the pH dependence of $\Phi_{NO_2^-}$ [14,17]. Daniels et al. [14] suggested that $HOONO_2$ was formed as an intermediate in the reaction of $O(^3P)$ and NO_3^-. This is unlikely as the $\Phi_{NO_2^-}$ values during irradiation with $\lambda > 280$ nm at alkaline pH are clearly significantly higher than those for $\Phi_O(^3P)$ (see Tables 2 and 4). Shuali et al. [15] suggested that a metastable isomer of NO_3^-, which reacts with either NO_2^- or NO_3^- depending on its state of dissociation, is responsible for the pH dependence of $\Phi_{NO_2^-}$. Bayliss and Bucat [17] suggested that it was due to the protonation of $[NO_3^-]^*$ at low pH. Wagner et al. [13] postulated that the two steps observed by Daniels et al. [14] in the pH dependence of $\Phi_{NO_2^-}$ are due to the reactions of $O^{\bullet -}$ with H_2O and H^+ in the solvent cage, but this explanation seems highly unlikely.

The hypothesis of Barat et al. [15,64] was called into question after Plumb et al. [68] carried out a series of experiments on the UV-irradiation of alkali nitrate salts found on the surface of Mars. The aim of the authors was to develop a model that could account for the positive indications for life, which occurred in biology tests conducted during the Viking mission to Mars. The authors demonstrated that the

Table 3
Photolysis of nitrate: quantum yield of hydroxyl radical formation

$[NO_3^-]$ (mM)	$^\bullet OH$ Scavenger (technique)	λ (nm)	T (K)	pH	$\Phi_{(OH)}$ (%)	Reference
3	SCN^-	308	278	4.0–9.0	0.8 ± 0.1	[10]
	(laser photolysis)		298		1.7 ± 0.3	
			318		2.8 ± 0.3	
			353		3.6 ± 0.4	
10	IPA (HPLC)	305	295	5.6	0.92 ± 0.04	[19]
0.2–4.0	C_4H_9Cl (GC), $Hg(CH_3)$ (AAS), $C_6H_5NO_2$, $C_6H_5OCH_3$ (HPLC)	313	293	6.2–8.2	1.3 ± 0.2	[18]
			303		1.7 ± 0.3	
2–200	methanol, IPA, cyclopentane (IC,GC,HPLC)	254	298	4–12	9	[42]

Table 4
NO_3^- photolysis: atomic oxygen data

$[NO_3^-]$ (mM)	$O(^3P)$ scavenger	λ (nm)	T (K)	pH	$\Phi_{(O)}$ (%)	Reference
5–50	cyclopentene (GC)	305	295 ± 2	5.6	0.11 ± 0.3	[19]
2–200	cyclopentene (GC)	254	298	4–12	>0.1	[42]

calorimetric analysis, traditionally used to determine $\Phi_{NO_2^-}$ data for NO_3^- photolysis during the irradiation of solid and solution samples, was suspect. It was found that additional NO_2^- was generated during the decay of $ONOO^-$ when the solutions were diluted to neutral pH [40]. It was therefore concluded that many of the $\Phi_{NO_2^-}$ results reported during earlier studies of NO_3^- photolysis were flawed. Edwards and Plumb [40,41,63] proposed that $OONO^-$ was indeed responsible for the pH dependence of $\Phi_{NO_2^-}$ and that NO_2^- formation was the result either of thermal decay and/or photochemical decomposition of $OONO^-$.

$ONOO^-$ has subsequently been the focus of intense research by biochemists [66,69–103]. Beckman et al. [69] reported that $ONOO^-$ can be formed in vivo through the reaction of $NO^\bullet$ and $O_2^{\bullet -}$. These biochemical experiments [66,69–103] have provided considerable insight into the mechanism of NO_2^- and O_2 formation from $ONOO^-$. Radi et al. [79] proposed that a reaction between $ONOO^-$ and $^\bullet OH$ can lead to a brief period of O_2 formation during $ONOO^-$ decomposition [75]:

$$ONOO^- + {}^\bullet OH \rightarrow ONOO^\bullet + OH^- \quad k_{19} = 5 \times 10^9\,M^{-1}\,s^{-1} \tag{19}$$

Decomposition of $ONOO^\bullet$ was reported to lead to O_2 generation with both the O atoms coming from NO_3^-:

$$ONOO^\bullet \rightarrow NO^\bullet + O_2 \tag{20}$$

Since $ONOO^-$ is reasonably stable in solution at $pH > 7$, while HOONO isomerizes rapidly to NO_3^- via reaction (18) [65], reaction (19) is more likely to occur at alkaline pH and could therefore cause the observed pH dependence of $\Phi_{NO_2^-}$. During NO_3^- photolysis, the $^\bullet OH$ that escapes the solvent cage in reaction (15) would initially react primarily with $ONOO^-$ in reaction (19), since NO_3^- is not an efficient $^\bullet OH$ scavenger ($k < 1.0 \times 10^5\,M^{-1}\,s^{-1}$ [104]). The $NO^\bullet$ formed in reaction (20) could then react with the $NO_2^\bullet$ formed in reaction (15). Mark et al. [42] recently proposed that the mechanism of NO_2^- formation during irradiation at 254 nm is reactions (7), (8), (15)–(17), (19), and (20). The authors discounted the hypothesis of Edwards and Plumb [40] that photolysis of $ONOO^-$ could lead to NO_2^- formation. Mark et al. [42] claimed that $ONOO^-$ is not photolyzed significantly at pH 13, since they obtained a $ONOO^-$ yield vs. UV-dose plot that was curved downwards only very slightly.

Mark et al. [42] pointed out that oxidation of $OONO^-$ by $NO_2^\bullet$ is also thermodynamically feasible. Recent research by Goldstein et al. [94] appears to rule this pathway out, however, since this reaction was not observed during a pulse radiolysis study. Mark et al. [42] claimed that their ability to identify $NO^\bullet$ in electron paramagnetic resonance (EPR) spin trapping experiments was direct evidence for reactions (19) and (20). This is not the case, since there could also be significant $NO^\bullet$ formation due to the photolysis of the NO_2^- which is formed over the extended course of NO_3^- photolysis. Recent $ONOO^-$ laser flash photolysis and pulse radiolysis studies of Kissner et al. [87] have since provided direct experimental evidence that reactions (7), (8), (19) and (20) do indeed lead to the formation of O_2 and NO_2^-. A subsequent radiolysis study by Goldstein et al. [94,105] suggests that a reaction between N_2O_3 and $ONOO^-$ could also compete with reaction (8) between pH 6 and 12:

$$N_2O_3 + ONOO^- \rightarrow NO_2^- + 2\,NO_2^\bullet \tag{21}$$

At lower pH, HOONO does not react with N_2O_3 while at higher pH the hydrolysis of N_2O_3 is base-catalyzed. Mark et al. [42] found that $\Phi_{NO_2^-}$ decreases as the photon flux increases which suggests that a second-order radical–radical recombination is also taking place. The authors proposed that the following reaction is important at high photon fluxes:

$$NO_2^\bullet + ONOO^\bullet + H_2O \rightarrow 2\,NO_3^- + 2\,H^+ \tag{22}$$

The $NO^{\bullet}$ formed in reaction (20) could also react with $^{\bullet}OH$ in reaction (5) to form HONO, since a combination of reactions (5), (9), (10), (15)–(17), (19) and (20), would satisfy the overall stoichiometry. This is much less likely to occur under most experimental conditions, however, since reactions (6) and (19) will greatly reduce the steady state concentration of $^{\bullet}OH$ relative to that of $NO_2^{\bullet}$.

3.2. *UV-dose dependence of* $\Phi_{NO_2^-}$

The mechanism responsible for NO_2^- formation during NO_3^- photolysis is further complicated by the fact that $\Phi_{NO_2^-}$ is not independent of the UV-dose at neutral and acidic pH. Daniels et al. [14] found that the rate of NO_2^- generation decreases sharply to an apparently constant residual rate during irradiation at pH 6 and $\lambda > 300$ nm. Addition of NO_2^- to the solution prior to photolysis slows the initial rate to the level observed if that concentration had been generated during the course of the photolysis [14,42]. The initial rate is dependent on the NO_3^- concentration, while the residual rate is independent of both the NO_2^- and NO_3^- concentrations [14]. This indicates that two separate pathways result in the formation of NO_2^- and that the major pathway is self-inhibiting as NO_2^- reacts with one of its precursors. In alkaline solutions, the NO_2^- concentration vs. UV-dose plot becomes almost linear [14,42]. Mark et al. [42] and Shuali et al. [15] observed similar results during irradiation at 254 and 229 nm, respectively. NO_2^- is a very efficient $^{\bullet}OH$ scavenger, so NO_2^- formation via reactions (7), (8), (15)–(17), (19) and (20) becomes less likely as the concentration of NO_2^- increases. The initial rate is dependent on the concentration of NO_3^-, since that will determine the steady-state concentration of HOONO. The residual reaction observed by Daniels et al. [16] at elevated NO_2^- concentrations was probably due to the reaction of $O(^3P)$ with NO_3^- possibly via peroxynitrate (O_2NOO^-) [24]:

$$O(^3P) + NO_3^- \rightarrow O_2NOO^- \rightarrow NO_2^- + O_2 \quad k_{23} = 3 \times 10^8\ M^{-1}\ s^{-1} \tag{23}$$

It should be noted that $O(^3P)$ can also react with NO_2^- to form NO_3^- [24]:

$$O(^3P) + NO_2^- \rightarrow NO_3^- \quad k_{24} = 3 \times 10^9\ M^{-1}\ s^{-1} \tag{24}$$

Daniels et al. [16] proposed that competition between reactions (23) and (24) is responsible for the self-inhibition of NO_2^- formation during extended photolysis. Since the yield of NO_2^- was typically $< 100\ \mu M$ in 1 M NO_3^- solutions, reaction (24) could not have been a significant factor in their experiments. Recent experiments on the wavelength dependence of $\Phi_{NO_2^-}$ during irradiation with a broad band source [106] during UV/H_2O_2 AOT treatments of tetrahydrofuran have provided strong evidence that NO_2^- formation from $O(^3P)$ is a significant reaction pathway during irradiation at $\lambda > 280$ nm. A combination of reactions (14) and (23) satisfies the overall stoichiometry of NO_3^- photolysis.

3.3. *The effect of* $^{\bullet}$*OH scavengers on* $\Phi_{NO_2^-}$

The addition of a variety of $^{\bullet}OH$ scavengers has been found to cause a substantial increase in $\Phi_{NO_2^-}$ during NO_3^- photolysis experiments carried out at pH < 9 in deionized water [13]. No increase was observed at more alkaline pH [14,42]. The most straightforward explanation for this would be that the $^{\bullet}OH$ scavengers eliminate the bulk recombination reaction between $^{\bullet}OH$ and $NO_2^{\bullet}$ in reaction (17), since the HOONO formed would otherwise isomerize to NO_3^- via reaction (18). The excess $NO_2^{\bullet}$ would react to form additional NO_2^- via reactions (9) and (10). The presence of the relatively stable $ONOO^-$ at alkaline pH greatly slows the rate of reaction (18), so the impact of the scavengers is less marked. $^{\bullet}OH$ scavengers also protect the NO_2^- and $ONOO^-$ generated during NO_3^- photolysis from attack by $^{\bullet}OH$ via reactions (6) and (19) [42].

Mark et al. [42] proposed detailed reaction mechanisms to account for the effect of methanol and cyclopentane on $\Phi_{NO_2^-}$ during irradiation at $\lambda = 254$ nm between pH 4 and 12. $^{\bullet}OH$ abstracts a hydrogen from cyclopentane to form the cyclopentyl radical, which was reported to react in the absence of O_2 with $NO_2^{\bullet}$ at pH 5 to form nitrocyclopentane and with $ONOO^-$ and $NO_2^{\bullet}$ at pH 9 to form cyclopentylnitrate. When cyclopentane was replaced by methanol $\Phi_{NO_2^-}$ increased at alkaline pH as hydrogen abstraction by $^{\bullet}OH$ results in the formation of the hydroxymethylperoxyl radical, which reacts with OH^- to form HCHO and $O_2^{\bullet -}$. reaction between $O_2^{\bullet -}$ and $NO_2^{\bullet}$ was reported to result in the formation O_2 and NO_2^- possibly via peroxynitrate (O_2NOO^-):

$$NO_2^{\bullet} + O_2^{\bullet -} \rightarrow O_2 + NO_2^- \quad k_{25} = 1 \times 10^8\ M^{-1}\ s^{-1} \tag{25}$$

Below pH 5, the hydroxymethylperoxyl radical reacts with $NO_2^{\bullet}$ to form HCHO and O_2NOO^- which then decomposes to form NO_2^- and O_2 [107].

3.4. *HOONO as a potential source of* $^{\bullet}$*OH*

A variety of different mechanisms have been proposed for reaction (18) (Scheme 3) to account for the presence of a strong oxidant which is formed as an intermediate. In 1970, Mahoney [67] claimed, on the basis of a kinetic study of reaction (18) in the presence of H_2O_2, that the homolysis of HOONO results in a 32% yield of $^{\bullet}OH$. Reactivity similar to that of $^{\bullet}OH$ has also been observed in recent biochemical experiments during the decay of HOONO in reaction (18) [69,72–78,81,83,84,108–110]. Koppenol et al. [80] subsequently claimed, however, that the available thermochemical and kinetic data was not consistent with either homolysis or heterolysis of HOONO. They proposed instead that an activated form of the '*trans*' isomer of HOONO is the oxidant (HOONO* in Scheme 3) [82]. In many of the initial biochemical studies it was argued that the reactivity of $ONOO^-$ could best be understood in terms of planar

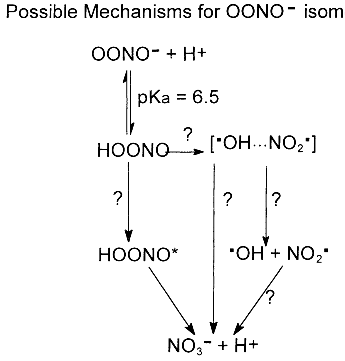

Scheme 3. Proposed mechanisms for the isomerization of HOONO to NO_3^- via reaction (18). Caged radical pairs are indicated by square brackets.

'*cis*' and '*trans*' isomers [80–82] based on the results of MOPAC computer modeling studies [80]. It was suggested that the '*cis*' form of $ONOO^-$ is energetically favored and is relatively stable in solution [82] and that reaction (18) occurs only via the '*trans*' isomer [81]. Protonation to form HOONO was believed to reduce the barrier between the '*cis*' and '*trans*' isomers, so that both isomers could exist in solution [80–82].

Merényi and Lind [71,111], Bartberger et al. [73] and Lymar and Hurst [75] have recently reported calculations which indicate that the approach used by Koppenol et al. [80] was incorrect and that the available thermochemical data are in fact consistent with homolysis. Lymar and Hurst [75] have reported ab initio calculations, which suggest that the '*cis*' and '*trans*' isomers are almost isoenergetic. If this is correct, there should be no major difference in the reactivity of these isomers. Merényi et al. [74] recently outlined several examples of experimental data that are consistent with homolysis. However, there is still very strong experimental evidence that suggests that $^{\bullet}OH$ formation does not occur [83–86,88,89,103,112]. Some $^{\bullet}OH$ scavengers do not reduce the reactivity of HOONO in vivo to the extent that would be anticipated on the basis of the known $^{\bullet}OH$ rate constants. For example, mannitol and benzoate do not protect α-1-proteinase or thiols from attack by HOONO at physiological pH [84,85]. Goldstein and Czapski [103] also found that the rate of oxidation of ferrocyanide in the presence of $ONOO^-$ was unaffected by the addition of formate ions and methanol at concentrations which would normally be sufficient to scavenge $^{\bullet}OH$. These authors subsequently decided that despite this the weight of the evidence supports $^{\bullet}OH$ formation. Squadrito and Pryor [77] recently postulated that an unusually stable long-lived $^{\bullet}OH$ and $NO_2^{\bullet}$ caged radical pair (see Scheme 3), which does not dissociate significantly, could account for the experimental data obtained during $^{\bullet}OH$ scavenger experiments.

Mark et al. [42] claimed, based on an experiment in which an alkaline $ONOO^-$ solution was added to a solution containing methanol at pH 4, that 10% of the HOONO formed during NO_3^- photolysis, homolyses to form $NO_2^{\bullet}$ and $^{\bullet}OH$. The authors mentioned the controversy over whether homolysis occurs during reaction (18) but offered no alternative explanation for the selectivity of the reactions with $^{\bullet}OH$ scavengers observed in $ONOO^-$ biochemical experiments [83–86,88,89,103]. Pfeiffer et al. [90] have reported that no NO_2^- is formed during the decay of HOONO at $pH < 5$ in biochemical experiments, while a 30% yield can be obtained at pH 7. The presence of $OONO^-$ therefore appears to be required for NO_2^- to be formed, possibly due to the formation of an adduct between the two species [87]. During NO_3^- photolysis at $pH < 5$, however, the $^{\bullet}OH$ that escapes the solvent cage in reaction (15) is thought to react with HOONO in reaction (19). It is difficult to see why this would not also happen during reaction (18) if, as Mark et al. suggested [42], a significant portion of $^{\bullet}OH$ does escape the solvent cage.

The $\Phi_{NO_2^-}$ experimental data reported for NO_3^- photolysis in the presence of $^{\bullet}OH$ scavengers have not always been consistent with the known $^{\bullet}OH$ rate constants. Bayliss and Bucat [17] found that the addition of 1 M NaBr doubled the rate of NO_2^- formation at pH 2.8 during irradiation at $\lambda = 254$ nm, while the addition of 0.05 M $NaAsO_2$ resulted in an increase of over 30 fold. The rate constants of the reactions of Br^- and AsO_2^- with $^{\bullet}OH$ are 1.1×10^{10} and $9.0 \times 10^9\ M^{-1}\ s^{-1}$, respectively [62]. Daniels et al. [14] obtained similar results and suggested that scavenging of the caged radical pair produced in reaction (15) was taking place. More research is clearly needed before any assumptions can be made concerning the exact nature of the oxidant formed as an intermediate during reaction (18).

3.5. The pH dependence of $\Phi_{NO_2^-}$

Daniels et al. [14] found that $\Phi_{NO_2^-}$ rises rapidly toward high pH in two steps for pH 8–10 and then for pH 11–13 during irradiation at 300 nm. Mark et al. [42] and Shuali et al. [15] observed similar results during irradiation at $\lambda < 280$ nm. It now seems clear that the first step is related to the stability of $OONO^-$ in solution. The second was almost certainly related to reaction (4). Mark et al. [42] proposed that the major pathway for NO_2^- formation at alkaline pH is reactions (7), (8), (15)–(17), (19) and (20) and assumed that there is no significant photolysis of $ONOO^-$. It is difficult to reconcile these assumptions with the results of Shuali et al. [15], Løgager and Sehested [65] and Plumb et al. [63], who explored the impact of using non-monochromatic light sources rather than a fixed $\lambda = 254$ nm source.

Shuali et al. [15] reported significant photobleaching of $ONOO^-$ generated in their NO_3^- photolysis experiments and proposed that the low-energy lines ($229\ nm < \lambda < 360\ nm$) of their Cd lamp were responsible. When a Pyrex® filter was used to exclude $\lambda < 290$ nm, $ONOO^-$ was completely eliminated from solution. Løgager and Sehested [65] also reported that the influence of $ONOO^-$ photolysis was severe at $pH > 9$ and that the rate of $ONOO^-$ decomposition varied significantly when 230, 280 and 305 nm cut-off filters were used. Plumb et al. [63] observed net $ONOO^-$ formation during the UV-irradiation of alkali nitrate salts at 254 nm, the irradiating wavelength used by Mark et al. [42]. Irradiation at 300 nm was found to result in photobleaching of $ONOO^-$ via a first-order process that results in isomerization to $NO_3{}^-$. Plumb et al. [63] developed a model to account for the steady state concentrations of $NO_2{}^-$ and $ONOO^-$ formed during irradiation of alkali nitrate salts at 254 nm. It was proposed that irradiation of $ONOO^-$ results either in the formation of $NO_2{}^-$ and $O(^3P)$:

$$ONOO^- \xrightarrow{h\nu} NO_2{}^- + O(^3P) \qquad (26)$$

or in photobleaching via isomerization to $NO_3{}^-$. The authors [40] postulated that O_2 formation occurs via reactions (16), (26) and (23). It seems unlikely that $O(^3P)$ can play a major role in $NO_2{}^-$ formation at alkaline pH in aqueous solution. Shuali et al. [15] were unable to detect $O(^3P)$ during $NO_3{}^-$ photolysis with $\lambda = 229$ nm and Mark et al. [42] reported that it could only play a very minor role, at best, in $NO_2{}^-$ formation at 254 nm.

Recent laser photolysis data reported by Kissner et al. [87] indicate that $O_2{}^{\bullet -}$ and $NO^\bullet$ are the major photolysis products of $ONOO^-$ during irradiation at 266 and 355 nm:

$$ONOO^- \xrightarrow{h\nu} NO^\bullet + O_2{}^{\bullet -} \qquad (27)$$

$$NO^\bullet + O_2{}^{\bullet -} \rightarrow ONOO^- \qquad (28)$$

The analogous formation of $HO_2{}^\bullet$ and $NO^\bullet$ was observed by Koch and Sodeau [113] during HOONO photolysis at 185 and 254 nm in low temperature matrices. It has been suggested that reaction (27) can even occur to a limited extent ($k_{27} = 0.02\ s^{-1}$) as a dark reaction at alkaline pH [71,74]. A combination of reactions (7), (8), (25) and (27) would result in the formation of $NO_2{}^-$ and O_2 during $NO_3{}^-$ photolysis. Since $ONOO^-$ absorbs strongly ($\varepsilon_{302} = 1670\ M^{-1}\ cm^{-1}$ [42]), this reaction pathway is likely to be a significant factor at alkaline pH during $NO_3{}^-$ photolysis.

Reaction (28) was found to result in almost quantitative regeneration of $ONOO^-$ in solution [87], so it seems unlikely that reactions (27) and (28) could result in a net change in the $ONOO^-$ concentration during the UV-irradiation of nitrate salts. Plumb et al. [63] did not investigate the question of whether the mechanism of the photobleaching reaction of $ONOO^-$ to form $NO_3{}^-$ is a direct unimolecular process via isomerization of an $ONOO^-$ excited state or a two step process involving:

$$ONOO^- \xrightarrow{h\nu} NO_2{}^\bullet + O^{\bullet -} \qquad (29)$$

$$NO_2{}^\bullet + O^{\bullet -} \rightarrow NO_3{}^- \qquad (30)$$

Merényi et al. [74] have proposed that reaction (29) occurs to a limited extent at alkaline pH even in the absence of incident light. The authors suggested that this reaction is responsible for the additional $NO_2{}^-$ formation observed by Plumb et al. [41] during their colorimetric analysis of $ONOO^-$. The reaction (29) would account for the fact that $NO_2{}^-$ is reported to reverse the inhibition of $^\bullet OH$ scavengers on O_2 formation during the decay of $ONOO^-$ at pH > 9 [75]. A combination of reactions (7), (9), (10), (21), (25), (27) and (29) would result in O_2 formation without requiring the involvement of $^\bullet OH$. If the rate of reaction (29) is photoenhanced during irradiation with $\lambda > 290$ nm, it could account for the data obtained by Shuali et al. [15] and Løgager and Sehested [65]. During $NO_3{}^-$ photolysis, reaction (29) would also clearly help to initiate formation of $NO_2{}^-$ via reactions (7), (8), (19) and (20). The extent to which $NO_2{}^-$ and O_2 are formed at alkaline pH via $ONOO^-$ photolysis and/or dark reactions via (26), (27) and (29) is a topic that requires further detailed investigation.

Recent biochemical research suggests that the reaction of $OONO^-$ with CO_2 can also be a significant degradation pathway for $ONOO^-$ [66,91–102,114,115]. An $ONOOCO_2{}^-$ adduct is formed, which may decompose to form a caged $CO_3{}^{\bullet -}$ and $^\bullet NO_2$ radical pair [73,75–77]. The controversy concerning this largely parallels that concerning reaction (18). Theoretical calculations appear to support homolysis [73,75] while some of the experimental data suggests that it is unlikely [76]. In the absence of an oxidizable substrate, $NO_3{}^-$ and CO_2 are the major products. Goldstein and Czapski [93] recently reported reactions in the presence of formate that result in the generation of O_2NOO^-. These reactions are similar to those proposed by Mark et al. [42] for $NO_2{}^-$ formation during $NO_3{}^-$ photolysis in the presence of methanol. $ONOOCO_2{}^-$ adduct formation would clearly be favored by the high $HCO_3{}^-$ concentrations in biological fluids. The possible impact of this reaction pathway during $NO_3{}^-$ photolysis at alkaline pH still has to be assessed.

3.6. Wavelength dependence of $\Phi_{NO_2{}^-}$

The proportion of light absorbed by the weak n → π^* band and the allowed π → π^* band appears to be the major factor determining the magnitude of $\Phi_{NO_2{}^-}$ during irradiation with a broad band light source (see Table 5). During irradiation into the forbidden n → π^* band, the $\Phi_{NO_2{}^-}$ is only 2.0% or less at pH 11.7. At shorter wavelengths, $\Phi_{NO_2{}^-}$ rises to values as high as 25% (see Table 2) due to reactions (7), (8), (16), (19) and (20). A sharp increase in $\Phi_{NO_2{}^-}$ was observed by Villars [116] at $\lambda < 280$ nm during irradiation of 0.33 M KNO_3 solutions at alkaline pH. Papée and Petriconi [43,44] observed $ONOO^-$ formation in alkaline $NO_3{}^-$ solutions when a Vycor® lamp sleeve was used with a 450 W Hg immersion lamp but not when it was replaced with a Corex® sleeve

Table 5
$NO_3{}^-$ photolysis: peroxynitrite data

$[ONOO^-]$ (mM)	technique	λ (nm)	T (K)	pH	$\Phi_{(ONOO^-)}$ (%)	Reference
2–200	UV–VIS	254	298	13	10	[42]

which filtered out $\lambda < 280$ nm. This lead to the suggestion that the wavelength dependence of $\Phi_{NO_2^-}$ was caused by $ONOO^-$ formation via reaction (16) at $\lambda < 280$ nm. Further evidence for this reaction was obtained by Mark et al. [42], who found that $\Phi_{NO_2^-}$ did not decrease significantly when 10 M isopropanol was present during NO_3^- photolysis at pH = 13 during irradiation at 254 nm. Therefore, since reaction (17) cannot be responsible for the bulk of the $ONOO^-$ formation at $\lambda < 280$ nm, there must be two pathways to $ONOO^-$ during NO_3^- photolysis. The fact that Φ_{ONOO^-} is much higher than $\Phi_O(^3P)$ rules out a process initiated by $O(^3P)$ formation via reaction (14) (see Tables 4 and 5) for reaction (16). $O(^1D)$ formation has been observed at $\lambda < 240$ nm during gas phase photolysis of HNO_3 [14,15,42,117]. If $O(^1D)$ were formed in solution, it might react with NO_2^- in the solvent cage to form $ONOO^-$. This appears to be unlikely, however, since H_2O_2 would be expected to be formed via the reaction of $O(^1D)$ and H_2O. H_2O_2 has not been observed as a significant product during NO_3^- photolysis during irradiation at $\lambda > 300$ nm [13]. It has therefore been proposed [13,17,41] that isomerization of the $^1\pi\pi^*$ excited state is the most likely explanation for the $ONOO^-$ formation observed at $\lambda < 280$ nm.

The Plumb et al. [63] model of $\Phi_{NO_2^-}$ data obtained during irradiation of nitrate salts suggests that reaction (16) does not occur at all at $\lambda > 280$ nm. Daniels et al. [14] claimed that $ONOO^-$ could not play a major role in the formation of NO_2^- during irradiation at $\lambda > 300$ nm, since they were unable to detect $ONOO^-$ ($\varepsilon_{302} = 1670\,M^{-1}\,cm^{-1}$ [42]) by UV-visible spectroscopy. Subsequent research by Shuali et al. [15], Løgager and Sehested [65] and Plumb et al. [63] has indicated, however, that $ONOO^-$ is photobleached from solution during irradiation at those wavelengths. As detection would therefore have been difficult under these circumstances, the presence of $ONOO^-$ cannot be discounted at $\lambda > 280$ nm on this basis. A combination of reactions (7), (8), (15), (17), (19) and (20) is therefore the most likely explanation for the initial UV-dose dependence in $\Phi_{NO_2^-}$ that was observed by Daniel's et al. [14] during irradiation at $\lambda > 300$ nm.

3.7. Temperature, wavelength and pH dependence of Φ_{OH}

The Φ_{OH} data for nitrite/nitrate photolysis reported in the literature are summarized in Tables 1 and 3. Zellner et al. [10] derived the following equations for the temperature dependence of Φ_{OH} based on the results reported for NO_2^- and NO_3^-:

$$\Phi_{OH}(T) = \Phi_{OH}(298\,K)\exp\left[(1560 \pm 480)\left(\frac{1}{298} - \frac{1}{T}\right)\right] \quad (NO_2^- \text{ photolysis}) \tag{31}$$

$$\Phi_{OH}(T) = \Phi_{OH}(298\,K)\exp\left[(1800 \pm 480)\left(\frac{1}{298} - \frac{1}{T}\right)\right] \quad (NO_3^- \text{ photolysis}) \tag{32}$$

The apparent activation energies are 13 ± 3 and 15 ± 4 $kJ\,mol^{-1}$, respectively. A significantly lower apparent activation energy of $6.29 \pm 0.33\,kJ\,mol^{-1}$ was calculated by Fischer and Warneck [22] for H_2O_2 from the literature values reported for reaction (1). The higher energy barrier associated with $^{\bullet}OH$ formation during NO_2^- and NO_3^- photolysis is thought to be related to the fact that $O^{\bullet -}$ rather than $^{\bullet}OH$ is formed in the initial photolysis step, since this would account for the significantly higher Φ_{OH} value seen during HONO photolysis [11,22]. Alif and Boule [11] and Fischer and Warneck [22] reported Φ_{OH} values of 45% and 35% for HONO photodecomposition (see Table 1). Fischer and Warneck [22] pointed out that Φ_{OH} for the photodissociation of HONO should be similar to that of H_2O_2 as the primary quantum yield value for photodecomposition in the gas phase is 100% for both molecules. Although a recent report claimed that Φ_{OH} rises from 100% at 300 nm to 180% at 250 nm in aqueous droplets in the atmosphere [118], Φ_{OH} is usually assumed to be close to 100% throughout this wavelength range [1,10].

In an analysis of the available experimental data (see Table 1) [8], Fischer and Warneck [22] have demonstrated that Φ_{OH} for NO_2^- photolysis rises from about 2% at 360 nm to a plateau of about 7% at 280 nm. These authors suggested that the wavelength dependence is due to the kinetic energy of the fragments produced on photodissociation. As the kinetic energy is higher at shorter wavelengths, the dissociation products should leave the solvent cage more easily. There appears to be a similar wavelength dependence during NO_3^- photolysis, since$\Phi_{^{\bullet}OH/O^{\bullet -}}$ rises from 1.3 ± 0.4% at $\lambda > 300$ nm at pH 4–9 [10] to 9% for $\Phi_{O^{\bullet -}}$ at 254 nm and pH 13 [42]. The accuracy of the latter value is questionable, as it may include contributions from $O^{\bullet -}$ formed from $ONOO^-$ and NO_2^- during the extended course of NO_3^- photolysis. $\Phi_{O^{\bullet -}}$ values are also not necessarily directly comparable to Φ_{OH}. Zellner et al. [10] found that Φ_{OH} for NO_2^- and NO_3^- photolysis at 308 nm is constant between pH 4 and 9 during irradiation at 308 nm (see Tables 1 and 3). An apparent drop in Φ_{OH} values at higher pH was thought to be due to a change in the effectiveness of SCN^- as an $^{\bullet}OH$ scavenger for the $^{\bullet}OH$ formed in reaction (15).

4. The impact of nitrite/nitrate photolysis in natural waters

Hamilton [119], Zafiriou [26] and Zepp and coworkers [27,120] were the first to recognize nitrite/nitrate photolysis as a potential source of $^{\bullet}OH$ in natural waters. In the early 1980's, Korte and coworkers [28,121] pointed out that nitrite/nitrate photolysis could have a depolluting influence through the oxidation of organic compounds. The authors calculated that the steady-state concentration of $^{\bullet}$OH was 5×10^{-16} M in natural waters containing 5–50 ppm NO_3^- and that the half-lives of typical organic chemicals were in the 80–400 h range. Haag et al. [30] concluded that the steady-state concentration of $^{\bullet}$OH in noon summer sunlight at the surface of a lake in Switzerland was 2×10^{-16} M. Zepp et al. [18] later calculated that Φ_{OH} was $1.3\pm0.2\%$ at 293 K at 313 nm using a variety of $^{\bullet}$OH scavengers. The authors concluded, based on the concentrations of NO_3^- (0.1 mM) and dissolved organic compounds (4 ppm), that most of the $^{\bullet}$OH production observed was due to NO_3^- photolysis. It was calculated that under these conditions most organic chemicals would have half-lives in the 500–4000 h range in noon summer sunlight. In a study of the environmental fate of industrial silicone fluids, Buch et al. [29] demonstrated that $^{\bullet}$OH radicals, generated in rivers and estuaries via nitrite/nitrate photolysis in sunlight, react with water soluble dimethylsiloxanols to form silicic acid and carbon dioxide. Kolpin and Kalkhoff [122] have studied the impact of nitrate-mediated $^{\bullet}$OH radical reactions on the environmental fate of atrazine, a widely used pesticide, in an Iowa stream.

Mopper and Zhou [31] used the approach of Zepp et al. [18] to study the impact of nitrite/nitrate photolysis in seawater. They concluded that the steady-state concentration of $^{\bullet}$OH is significantly lower than in comparable freshwater samples due to reaction between $^{\bullet}$OH and Br^-. The $^{\bullet}$OH concentration ranged from around 1.1×10^{-18} M in open-ocean surface water ($[NO_3^-]=0.05\,\mu$M, $[NO_2^-]=0\,\mu$M) to 2.6×10^{-17} M in upwelled coastal waters ($[NO_3^-]=15\,\mu$M, $[NO_2^-]=1\,\mu$M). NO_2^- and NO_3^- photolysis was calculated to be responsible for 7 and 35% of $^{\bullet}$OH production in the coastal water but less than 1% combined in the open ocean surface water in the Sargasso Sea. The remainder of the $^{\bullet}$OH production was reported to be due to the photolysis of dissolved organic matter. Torrents et al. [38] have studied NO_3^- photolysis mediated degradation of atrazine in Chesapeake Bay. Research has also focused on the role of OH$^{\bullet}$ and $NO_x^{\bullet}$ in the atmosphere [10,21,32,33,37,123–125]. HONO is formed at night in the gas phase primarily through the reaction of $NO_2^{\bullet}$ and H_2O and is photolyzed by sunlight to form the $^{\bullet}$OH radical [21,32,37,126]. Recent research has focused on the formation of $^{\bullet}$OH radicals from nitrite/nitrate photolysis within aqueous droplets in the troposphere [21,33,108,125].

5. Reaction of nitrite/nitrate photolysis intermediates with organic pollutants

Bilski et al. [9] have used EPR spin trapping with DMPO and nitromethane to characterize the secondary radicals generated from organic and inorganic substrates during NO_2^- photolysis at 360 nm in aqueous solution. The authors identified a variety of organic and inorganic radicals and concluded, based on the high rate of oxygen consumption by organic substrates, that photooxidation initiated by NO_2^- photolysis could potentially lead to the destruction of organic pollutants. The reactions of organic pollutants initiated by nitrite/nitrate photolysis can involve photonitration or photonitrosation [34–36,46–56,127,128]. A potential problem associated with nitrite/nitrate photolysis is that the nitration and nitrosation reactions of polycyclic aromatic compounds, such as biphenyls, can result in the formation of highly mutagenic and carcinogenic compounds [34–36,46–52,129]. Japanese researchers [34–36,46–48] have studied the nitration, nitrosation, hydroxylation and oxidation reactions of polycyclic aromatic hydrocarbons (PAHs) in the environment. Studies by Suzuki et al. [36] have suggested that reactions initiated by nitrite/nitrate photolysis in natural waters could be a viable pathway for generating nitro-PAHs which are known to be particularly strong mutagens [52].

Research by Bunce [128] and Boule [11,53–56] has focused on the mechanism of the hydroxynitration of aromatic organic compounds during nitrite/nitrate photolysis in aqueous solution. Niessen et al. [53] obtained a combined quantum yield of $0.6\pm0.15\%$ for the products generated through the indirect phototransformation of phenol during prolonged photolysis of a 10 mM KNO_3 solution at pH = 5.2 in the 290–350 nm range. Nitration and nitrosation reactions result in the formation of 2-nitrophenol, 4-nitrophenol, 4-nitropyrocatechol and 4-nitrosophenol. Boule and coworkers [11,53–56] have found that, in the case of monochlorophenols and nitrophenols, only *o*- and *p*-hydroxylation products (with respect to -OH) are formed. The electron withdrawing character of the -Cl and $-NO_2$ appears to hinder the nitration and nitrosation reactions. The hydroxylation and nitrosation reactions observed during NO_2^- photolysis are clearly the result of $^{\bullet}$OH and NO$^{\bullet}$ formed in reaction (3). Boule and coworkers [11] have proposed that reactions involving $^{\bullet}$OH, $^{\bullet}NO_2$ and N_2O_3 are responsible for the hydroxylation, nitration and nitrosation reactions observed during NO_2^- photolysis. This hypothesis will have to be re-evaluated in light of the recent biochemical research on the oxidation reactions of $OONO^-$ and the $ONOOCO_2^-$ adduct [66,91–102,115]. Lemercier et al. [66] and Uppu et al. [100,115] recently reported detailed studies of the reactions of phenol during the dark decay of $OONO^-$. They concluded that the oxidant formed as an intermediate during reaction (18) is responsible for hydroxylation and the $ONOOCO_2^-$ adduct is responsible for nitration and nitrosation reactions. It should be noted these nitration reactions do not occur with all aromatic compounds, however. Zhang et al [130] have recently reported that nitration products were not observed during the dark reaction between HOONO and melatonin in the presence and absence of CO_2. A one electron oxidation involving HOONO results in the formation of a melatoninyl radical cation which then reacts with $^{\bullet}$OH and HOONO to form hydroxylated products or with $NO_2^{\bullet}$ and HOONO to form a pyrroloindole compound.

6. Impact of NO_3^- on the use of AOTs in drinking water and wastewater applications

Significant concentrations of NO_2^- and NO_3^- are often present in both waste and natural waters. The $^\bullet OH$ formed via NO_2^- and NO_3^- photolysis initiates degradative oxidation reactions of organic pollutants. NO_2^- and NO_3^- are therefore potential alternative sources of $^\bullet OH$ for use in AOTs during irradiation at $\lambda > 280$ nm where H_2O_2 absorbs weakly. Bilski et al. [12] have claimed based on an EPR study of radical intermediates that NO_2^- photolysis during irradiation at 360 nm could have a significant impact on the degradation of industrial contaminants. Our experimental work indicates that this is unlikely, however. Irradiation of 50 mM isopropanol solution ($k_{OH} = 1.9 \times 10^9\ s^{-1}$ [62]) in a UV-reactor fitted with a Pyrex® lamp sleeve in the presence of 10 mM NO_2^- and NO_3^-, resulted in <1% IPA degradation after 1 h [106]. Mark et al. [42] reported that a photoisomerization process results in the formation of $OONO^-$ with $\Phi = 10\%$ and $\Phi_{OH} = 9\%$, during NO_3^- photolysis at $\lambda = 254$ nm [42]. The HOONO and $^\bullet OH$ generated might be expected to initiate significant degradation of organic pollutants during irradiation from a broad band $\lambda > 200$ nm source. When 1 mM isopropanol solutions were irradiated in a UV-reactor with $\lambda > 200$ nm in the presence of 10 mM NO_2^- and NO_3^-, however, the rate of degradation increased only slightly when compared to direct UV-irradiation experiments [106]. The $NO_2^\bullet$ generated in reaction (15) results in the formation of NO_2^- via reaction (25). HOONO also reacts with $^\bullet OH$ to form additional NO_2^- via reactions (7), (8), (19) and (20). The rate of IPA degradation was therefore minimal, since NO_2^- and HOONO are both efficient $^\bullet OH$ scavengers.

One of the most serious drawbacks associated with NO_3^- photolysis during photochemically based AOTs is that the formation of NO_2^- can result in concentrations that exceed the legislated levels allowed in drinking water [131,132]. von Sonntag and Schuchmann [132] have demonstrated that during irradiation of 50 ppm NO_3^- solutions (the maximum level allowed under E.U. legislation) with $\lambda = 254$ nm and a UV-dose of 40 mJ cm^{-2}, the NO_2^- concentration does not exceed the maximum allowed level of 0.1 ppm. However, during the commercial UV/H_2O_2 treatment of waters containing organic pollutants, UV-doses are much higher and yields of NO_2^- can easily exceed 0.1 ppm [106]. Absorption by NO_3^- is very slight at 254 nm ($\varepsilon = 3\ M^{-1}\ cm^{-1}$) when compared to the major $\pi \rightarrow \pi^*$ absorption band at 200 nm ($\varepsilon_{max} = 9900\ M^{-1}\ cm^{-1}$). The formation of NO_2^- should therefore be monitored carefully in UV/H_2O_2 applications where there is a significant NO_3^- concentration.

Sörensen and Frimmel [133] have studied the irradiation of EDTA at 254 and 222 nm in 50 ppm NO_3^- solutions in the presence and absence of H_2O_2. NO_3^- was reported to cause a significant ‘inner filter’ effect by reducing absorption of UV by H_2O_2, which results in a significant reduction in the efficiency of UV/H_2O_2 systems. As the Φ_{OH} values for NO_2^- and NO_3^- photolysis are relatively low, the reduction in the rate of the oxidation reactions initiated by H_2O_2 photolysis should be greater than any increase resulting from nitrite/nitrate photolysis. Sörensen and Frimmel [133] did not consider the fact that $^\bullet OH$ formed during H_2O_2 photolysis can react with several of the intermediates formed during NO_3^-, such as HOONO and NO_2^-. Scavenging of $^\bullet OH$ by NO_2^- via reaction (6) will also reduce the rate of degradation from that expected on the basis of an ‘inner filter’ effect alone [106]. Scavenging of $^\bullet OH$ by NO_2^- is an important factor during the extended course of UV/H_2O_2 treatments in NO_3^- rich waters, particularly in instances where organic contaminants are poor $^\bullet OH$ scavengers and/or are present at very low concentrations. Alvarez et al. [107] reported that a reaction between H_2O_2 and $OONO^-$ can result in significant formation of O_2 and NO_2^- due to the formation of a transient complex between H_2O_2 and $OONO^-$. Clearly, the influence of NO_3^- is more complex than a simple ‘inner filter’ effect during UV/H_2O_2 treatments.

7. Conclusions

Neither NO_2^- nor NO_3^- photolysis represents a promising pathway for $^\bullet OH$ generation in AOTs. The reported Φ_{OH} values for NO_3^- photolysis are relatively low, rising from $1.3 \pm 0.4\%$ at around 300 nm to 9.0% at 254 nm (see Table 3). Values for NO_2^- photolysis increase from 1.5 to 8.0% between 350 and 250 nm. In contrast, Φ_{OH} during H_2O_2 photolysis is thought to be at least 100% throughout this wavelength range [1,10,21]. NO_2^- is a very efficient $^\bullet OH$ scavenger ($k = 1.0 \times 10^{10}\ s^{-1}$) and is therefore not expected to be a viable source of $^\bullet OH$. Since NO_3^- is a very poor $^\bullet OH$ scavenger ($k < 1.0 \times 10^5\ s^{-1}$ [62]), it would appear at first glance to be a more promising source of $^\bullet OH$ for AOTs. HOONO generated via reactions (16) and (17) reacts with $^\bullet OH$ to form O_2 and NO_2^-, however. The oxidant which is generated from HOONO as an intermediate during reaction (18), could potentially initiate the degradation of organic contaminant, but the viability of this reaction pathway is limited by the rapid isomerization of HOONO to NO_3^-.

During UV/H_2O_2 treatments, NO_2^- and NO_3^- can inhibit the degradation of organic contaminants via an ‘inner filter’ effect on absorption by H_2O_2, which has a significantly higher Φ_{OH}. Since the photolysis of NO_2^- and NO_3^- also results in the formation of a number of species that can react with H_2O_2 and $^\bullet OH$, the presence of NO_2^- and NO_3^- can significantly reduce the efficiency of photochemically based AOTs [106]. The formation of NO_2^- via NO_3^- photolysis must be carefully monitored in UV/H_2O_2 drinking water treatment applications. An understanding of the mechanism of NO_3^- photolysis has been used successfully to alleviate this problem by adjusting the wavelength profile of the incident light. The $\Phi_{NO_2^-}$ is lowered substantially without a major drop in the overall efficiency of UV/H_2O_2

treatment [106]. The potential formation of highly carcinogenic and mutagenic polycyclic aromatic intermediates via the nitration, nitrosation, and hydroxylation of these compounds during the prolonged course of NO_3^- photolysis, is a topic which may have to be studied carefully in future UV/H_2O_2 wastewater treatment applications.

Acknowledgements

This work was funded by a Natural Sciences and Engineering Research Council of Canada Collaborative Research and Development Grant with Calgon Carbon Corporation (CCC) of Markham, Ontario, Canada. The authors would like to thank Dr Mihaela Stefan (UWO) and Drs. Ali Safarzadeh-Amiri, Stephen R. Cater and Mr. Keith G. Bircher, P.E. (CCC) for their insight and assistance in various aspects of the project.

References

[1] J.R. Bolton, S.R. Cater, in: G. Heltz, R.G. Zepp, D. Crosby (Eds.), Surface and Aquatic Photochemistry, Lewis, Boca Raton, FL, 1994, p. 467.
[2] O. Legrini, E. Oliveros, A.M. Braun, Chem. Rev. 93 (1993) 671.
[3] S.J. Strickler, M. Kasha, J. Am. Chem. Soc. 85 (1963) 2899.
[4] E. Rotlevi, A. Treinin, J. Phys. Soc. 69 (1965) 2645.
[5] H.J. Maria, J.R. McDonald, S.P. McGlynn, J. Am. Chem. Soc. 95 (1973) 1050.
[6] M. von Grätzel, S. Taniguchi, A. Henglein, Ber. Bunsenges Ber. 74 (1970) 488.
[7] I. Wagner, H. Strehlow, Z. Phys. Chemie. Neue Folge 132 (1982) 151.
[8] O.C. Zafiriou, R. Bonneau, Photochem. Photobiol. 45 (1987) 723.
[9] P. Bilski, J. Szychlinski, E. Oleksy, J. Photochem. Photobiol. A: Chem. 44 (1988) 269.
[10] R. Zellner, M. Exner, H. Herrman, J. Atmos. Chem. 10 (1990) 411.
[11] A. Alif, P. Boule, J. Photochem. Photobiol. A: Chem. 59 (1991) 357.
[12] P. Bilski, C.F. Chignell, J. Szychlinski, A. Borkowski, E. Oleksy, K. Reszka, J. Am. Chem. Soc. 114 (1992) 549.
[13] I. Wagner, H. Strehlow, G. Busse, Z. Phys. Chemie. Neue Folge 123 (1980) 1.
[14] M. Daniels, R.V. Meyers, R.V. Belardo, J. Phys. Chem. 72 (1968) 389.
[15] U. Shuali, M. Ottolenghi, J. Rabani, Z. Yelin, J. Phys. Chem. 78 (1969) 3445.
[16] F. Barat, L. Gilles, J. Sutton, J. Chem. Soc. A (1970) 1982.
[17] N.S. Bayliss, R.B. Bucat, Aust. J. Chem. 28 (1975) 1865.
[18] R.G. Zepp, J. Hoigné, H. Bader, Environ. Sci. Technol. 21 (1987) 443.
[19] P. Warneck, C. Wurzinger, J. Phys. Chem. 92 (1988) 6278.
[20] E. Warburg, Sitzungsber. Preuss. Akad. Wiss., Phys-Math. Kl. 52 (1918) 1228.
[21] R. Zellner, H. Hermann, in: R.J.H. Clark (Ed.), Spectroscopy in Environmental Science, Wiley, New York, 1995, p. 381.
[22] M. Fischer, P. Warneck, J. Phys. Chem. 100 (1996) 18749.
[23] P.A. King, V.E. Anderson, J.O. Edwards, G. Gustafson, R.C. Plumb, J.W. Suggs, J. Am. Chem. Soc. 114 (1992) 5430.
[24] M.C. Gonzalez, A.M. Braun, Res. Chem. Intermed. 21 (1995) 837.
[25] M.C. Gonzalez, A.M. Braun, J. Photochem. Photobiol. A 93 (1996) 7.
[26] O.C. Zafiriou, J. Geophys. Res. 79 (1974) 4491.
[27] R.G. Zepp, D.M. Cline, Environ. Sci. Technol. 11 (1977) 359.
[28] H. Russi, D. Kotzias, F. Korte, Chemosphere 11 (1982) 1041.
[29] R.R. Buch, T.H. Lane, R.B. Annelin, C.L. Frye, Environ. Toxicol. Chem. 3 (1984) 215.
[30] W.R. Haag, J. Hoigné, Chemosphere 14 (1985) 1659.
[31] K. Mopper, X. Zhou, Science 250 (1990) 661.
[32] H. Akimoto, H. Takagi, F. Sakamaki, Int. J. Chem. Kinet. 13 (1981) 785.
[33] P. Warneck, Ber. Bunsenges. Phys. Chem. 96 (1992) 454.
[34] J. Suzuki, H. Okazaki, Y. Nishi, S. Suzuki, Bull. Environm. Contam. Toxicol. 29 (1982) 511.
[35] J. Suzuki, T. Hagino, S. Suzuki, Chemosphere 16 (1987) 859.
[36] J. Suzuki, T. Sato, A. Ito, S. Suzuki, Bull. Environ. Contam. Toxicol. 45 (1990) 516.
[37] G. Lammel, J.N. Cape, Chem. Soc. Rev. (1996) 361.
[38] A. Torrents, B.G. Anderson, S. Bilboulian, W.E. Johnson, C.J. Hapeman, Environ. Sci. Technol. 31 (1997) 1476.
[39] A. Treinin, E. Hayon, J. Am. Chem. Soc. 92 (1970) 5821.
[40] R.C. Plumb, J.O. Edwards, M.A. Hermann, Analyst 117 (1992) 1639.
[41] J.O. Edwards, R.C. Plumb, Prog. Inorg. Chem. 41 (1994) 599.
[42] G. Mark, H.-G. Korth, H.-P. Schuchmann, C. von Sonntag, J. Photochem. Photobiol. A 101 (1996) 89.
[43] H.M. Papée, G.L. Petriconi, Nature 204 (1964) 142.
[44] G.L. Petriconi, H.M. Papée, J. Inorg. Nucl. Chem. 30 (1968) 1525.
[45] G.L. Petriconi, H.M. Papée, Can. J. Chem. 44 (1966) 977.
[46] J. Suzuki, H. Okazaki, T. Sato, S. Suzuki, Chemosphere 11 (1982) 437.
[47] T. Ohta, J. Suzuki, Y. Iwano, S. Suzuki, Chemosphere 11 (1982) 797.
[48] J. Suzuki, T. Sato, S. Suzuki, Chem. Pharm. Bull. 33 (1984) 2507.
[49] J. Arey, B. Zielinska, R. Atkinson, A.M. Winer, T. Ramdahl, J. Pitts, Atmos. Environ. 20 (1986) 2339.
[50] B. Zielinska, J. Arey, R. Atkinson, P.A. McElroy, Environ. Sci. Technol. 23 (1989) 723.
[51] D. Nakajima, Y. Yoshida, J. Suzuki, S. Suzuki, Chemosphere 30 (1995) 409.
[52] K. Miyanishi, T. Kinouchi, K. Kataoka, T. Kanoh, Y. Ohnishi, Carcinogenesis 17 (1996) 1483.
[53] R. Niessen, D. Lenoir, P. Boule, Chemosphere 17 (1988) 1977.
[54] G. Schedel, D. Lenoir, P. Boule, Chemosphere 22 (1991) 1063.
[55] F. Machado, P. Boule, J. Photochem. Photobiol. A: Chem. 86 (1995) 73.
[56] J.-F. Pilichowski, P. Boule, J.-P. Billard, Can. J. Chem. 73 (1995) 2143.
[57] Y. Usui, S.M. Takebayashi, M. Takeuchi, Bull. Chem. Soc. Japan 65 (1992) 3183.
[58] H. Zeldes, R. Livingston, J. Am. Chem. Soc. 90 (1968) 4540.
[59] L.G. Forni, V.O. Mora-Arellano, J.E. Packer, R.L. Willson, J. Chem. Soc. Perkin Trans. II (1986) 1.
[60] U. Deister, P. Warneck, C. Wurzinger, Ber. Bunsenges. Phys. Chem. 94 (1990) 594.
[61] A. Alif, P. Boule, J. Lemaire, Chemosphere 16 (1987) 2213.
[62] G.V. Buxton, C.L. Greenstock, W.P. Helman, A.B. Ross, J. Phys. Chem. Ref. Data 17 (1988) 513.
[63] R.C. Plumb, J.O. Edwards, J. Phys. Chem. 96 (1992) 3245.
[64] F. Barat, B. Hickel, J. Sutton, Chem. Commun. (1969) 125.
[65] T. Løgager, K. Sehested, J. Phys. Chem. 97 (1993) 6664.
[66] J.-N. LeMercier, S. Padmaja, R. Cueto, G.L. Squadrito, R.M. Uppu, W.A. Pryor, Arch. Biochem. Biophys. 345 (1997) 160.
[67] L.R. Mahoney, J. Am. Chem. Soc. 92 (1970) 5262.
[68] R.C. Plumb, R. Tantayanon, M. Libby, W.W. Xu, Nature 338 (1989) 633.
[69] J.S. Beckman, T.W. Beckman, J. Chen, P.A. Marshall, B.A. Freeman, Proc. Natl. Acad. Sci. USA 87 (1990) 1620.
[70] W.H. Koppenol, R. Kissner, Chem. Res. Toxicol. 11 (1998) 87.
[71] G. Merényi, J. Lind, Chem. Res. Toxicol. 11 (1998) 243.
[72] G.L. Squadrito, W.A. Pryor, Free Radical Biol. Med. 25 (1998) 392.
[73] M.D. Bartberger, L.P. Olson, K.N. Houk, Chem. Res. Toxicol. 11 (1998) 710.

[74] G. Merényi, J. Lind, S. Goldstein, G. Czapski, Chem. Res. Toxicol. 11 (1998) 712.
[75] S.V. Lymar, J.K. Hurst, Chem. Res. Toxicol. 11 (1998) 714.
[76] W.H. Koppenol, Chem. Res. Toxicol. 11 (1998) 716.
[77] G.L. Squadrito, W.A. Pryor, Chem. Res. Toxicol. 11 (1998) 718.
[78] R. Radi, Chem. Res. Toxicol. 11 (1998) 720.
[79] R. Radi, J.S. Beckman, K.M. Bush, B.A. Freeman, J. Biol. Chem. 266 (1991) 4244.
[80] W.H. Koppenol, J.J. Moreno, W.A. Pryor, H. Ischiropoulos, J.S. Beckman, Chem. Res. Toxicol. 5 (1992) 834.
[81] J.P. Crow, C. Spruell, J. Chen, C. Gunn, H. Ischiropoulos, M. Tsai, C.D. Smith, R. Radi, W.H. Koppenol, J.S. Beckman, Free Radical Biol. Med. 16 (1994) 331.
[82] J.-H. Tsai, J.G. Harrison, J.C. Martin, T.P. Hamilton, M. van der Woerd, M.J. Jablonsky, J.S. Beckman, J. Am. Chem. Soc. 116 (1994) 4115.
[83] W.A. Pryor, X. Jin, G.L. Squadroto, Proc. Natl. Acad. Sci. USA 91 (1994) 11173.
[84] J.J. Moreno, W.A. Pryor, Chem. Res. Toxicol. 5 (1992) 425.
[85] C. Quijano, B. Alvarez, R.M. Gatti, O. Augusto, R. Radi, Biochem. J. 322 (1997) 167.
[86] J.S. Beckman, W.H. Koppenol, Am. J. Phys. 271 (1996) C1424–C1437.
[87] R. Kissner, T. Nauser, P. Bugnon, P.G. Lye, W.H. Koppenol, Chem. Res. Toxicol. 10 (1997) 1285.
[88] M. Narayan, L.J. Berliner, A.J. Merola, P.T. Diaz, T.L. Clanton, Free Radical Res. 27 (1997) 63.
[89] N.W. Kooy, J.A. Royall, H. Ischiropolous, Free Radical Res. 27 (1997) 245.
[90] S. Pfeiffer, A.C.F. Gorren, K. Schmidt, E.R. Werner, B. Hansert, D.S. Bohle, B. Mayer, J. Biol. Chem. 272 (1997) 3465.
[91] S. Padmaja, G.L. Squadrito, J.-N. LeMercier, R. Cueto, W.A. Pryor, Free Radical Biol. Med. 23 (1997) 917.
[92] S.V. Lymar, J.K. Hurst, Inorg. Chem. 37 (1998) 294.
[93] S. Goldstein, G. Czapski, J. Am. Chem. Soc. 120 (1998) 3458.
[94] S. Goldstein, A. Saha, S.V. Lymar, G. Czapski, J. Am. Chem. Soc. 120 (1998) 5549.
[95] A. Gow, D. Duran, S.R. Thom, H. Ischiropoulos, Arch. Biochem. Biophys. 333 (1996) 42.
[96] A. Denicola, B.A. Freeman, M. Trujillo, R. Radi, Arch. Biochem. Biophys. 333 (1996) 49.
[97] S.V. Lymar, Q. Jiang, J.K. Hurst, Biochemistry 35 (1996) 7885.
[98] S.V. Lymar, J.K. Hurst, J. Am. Chem. Soc. 117 (1995) 8867.
[99] S.V. Lymar, J.K. Hurst, Chem. Res. Toxicol. 9 (1996) 845.
[100] R.M. Uppu, G.L. Squadrito, W.A. Pryor, Arch. Biochem. Biophys. 327 (1996) 335.
[101] W.A. Pryor, J.-N. LeMercier, H. Zhang, R.M. Uppu, G.L. Squadrito, Free Radical Biol. Med. 23 (1997) 331.
[102] S. Goldstein, G. Czapski, Inorg. Chem. 36 (1997) 5113.
[103] S. Goldstein, G. Czpaski, Nitric Oxide 1 (1997) 417.
[104] R.E. Huie, P. Neta, J. Phys. Chem. 90 (1986) 1193.
[105] S. Goldstein, G. Czapski, J. Lind, G. Merényi, Chem. Res. Toxicol. 12 (1999) 132.
[106] J. Mack, A. Safarzadeh-Amiri, S.R. Cater, J.R. Bolton, J. Adv. Oxid. Technol. (1999), submitted for publication.
[107] B. Alvarez, A. Denicola, R. Radi, Chem. Res. Toxicol. 8 (1995) 859.
[108] T. Arakaki, T. Miyake, M. Shibata, H. Sakugawa, Nippon Kagaku Kishi 9 (1998) 619.
[109] G. Yang, T.E.G. Candy, M. Boaro, H.E. Wilkin, P. Jones, N.B. Nazhat, R.A. Saadalla-Nazhat, D.R. Blake, Free Radical Biol. Med. 12 (1992) 327.
[110] J.S. Beckman, H. Ischiropoulos, L. Zhu, M. van der Woerd, C. Smith, J. Chen, J. Harrison, J.C. Martin, M. Tsai, Arch. Biochem. Biophys. 298 (1992) 438.
[111] G. Merényi, J. Lind, Chem. Res. Toxicol. 10 (1997) 1216.
[112] S. Goldstein, G.L. Squadrito, W.A. Pryor, G. Czapski, Free Radical Biol. Med. 21 (1996) 965.
[113] T.G. Koch, J.R. Sodeau, J. Phys. Chem. 99 (1995) 10824.
[114] R.M. Uppu, G.W. Winston, W.A. Pryor, Chem. Res. Toxicol. 10 (1997) 1331.
[115] R.M. Uppu, J.-N. LeMercier, G.L. Squadrito, H. Zhang, R.M. Bolzan, W.A. Pryor, Arch. Biochem. Biophys. 358 (1998) 1.
[116] D.S. Villars, J. Am. Chem. Soc. 49 (1927) 326.
[117] A.A. Turnipseed, G.L. Vaghjiani, J.E. Thompson, A.R. Ravishankara, J. Chem. Phys. 96 (1992) 5887.
[118] H.-J. Benkelberg, A. Schäfer, P. Warneck, in: K.H. Becker (Ed.), Eurotrac: Atmospheric Oxidation Processes, 25–27 September 1990, Madrid, Spain, Air Pollution Research Report 33, CEC, Brussels, 1991, p. 130.
[119] R.D. Hamilton, Limnol. Oceanogr. 9 (1964) 107.
[120] O.C. Zafiriou, J. Joussot-Dubien, R.G. Zepp, R.G. Zika, Environ. Sci. Technol. 18 (1984) 358A.
[121] D. Kotzias, H. Parlar, F. Korte, Naturwissenschaften 69 (1982) 444.
[122] D.W. Kolpin, S.J. Kalkhoff, Environ. Sci. Technol. 27 (1993) 134.
[123] W.P. Carter, A.M. Winer, R. Atkinson, J. Pitts, Int. J. Chem. Kinet. 13 (1981) 785.
[124] W.P. Carter, R. Atkinson, J. Pitts, Int. J. Chem. Kinet. 14 (1982) 1071.
[125] M. Exner, H. Hermann, R. Zellner, Ber. Bunsenges. Phys. Chem. 96 (1992) 470.
[126] M. Ammann, M. Kalberer, D.T. Jost, L. Tobler, E. Rossler, D. Piguet, H.W. Gaggeler, U. Baltensperger, Nature 395 (1998) 157.
[127] D. Williams, H. Lyn, Nitric Oxide 1 (1997) 522.
[128] N.J. Bunce, S.R. Cater, J.M. Wilson, J. Chem. Soc. Perkin Trans. II (1985) 2013.
[129] E. Halfpenny, P.L. Robinson, J. Chem. Soc. (1952) 928.
[130] H. Zhang, G.L. Squadrito, W.A. Pryor, Biochem. Biophys. Res. Commun. 251 (1998) 83.
[131] H. Bernhardt, O. Hoyer, K. Kick, D. Schoenen, J. Gebel, B. Hengesbach, A. Kolch, P. Karanis, H. Rüden, C. von Sonntag, H.-P. Schuchmann, Wasser Abwasser 135 (1994) 677.
[132] C. von Sonntag, H.-P. Schuchmann, J. Water Supply Res. Techol. Aqua. 41 (1992) 67.
[133] M. Sörensen, F.H. Frimmel, Wat. Res. 31 (1997) 2885.